ISBN: 978-3-95450-229-5 ISSN: 2673-5520 doi:10.18429/JACoW-MEDSI2020-WEPA09

A NEW THREE-SIGNAL 2D-BEAM-POSITION-MONITOR BASED ON A SEGMENTED IONIZATION CHAMBER

M. Goerlitz*, W. A. Caliebe, DESY, Hamburg, Germany

Abstract

At DESY in 2020 a three-signal beam position monitor (BPM) was constructed, which is based on a Ionization Chamber design with split up electrodes. It is using three signals to determinate horizontal and vertical positions of a x-ray beam. The relation between signals and position can be described by a multiple linear regression (MLR). The calibration is done by linear optimization algorithms, which are described in detail, especially to give an engineering-based resume, which can easily applied to other systems. The results of the solution will be compared and discussed.

INTRODUCTION AND MOTIVATION

Due to the facts that synchrotron x-ray beam sizes are getting smaller and more experiments demand a focussed beam, the necessity of a controlled stable beam increases. Some demands of monitoring devices are, that they should not absorb significantly x-ray intensity, do not lead to bragg peaks on x-ray cameras, nor have a large signal to noise ratio. Most available transmissive BPMs are based on: (1) depositioned segmented diamond windows [1,2] with measurement ranges in the µm-region and fast acquisition times. (2) two 90°-turned ionization chambers with split up electrodes [3,4], wherefore the measuring range is in the mm-range. They have in common that they need four raw signals to calculate a 2D-position xy-location. A conventional ionization chamber at a synchrotron beamline consists of two plates, which are arranged parallel to each other and give one signal. They have the advantage to measure at low as well as high energies, whereas the absorption can be adjusted by using heavier gas like Krypton for higher energies or Nitrogen for lower energies [5].

The new evaluated design of a beam position ionization chamber is based on three signals.

MATERIAL AND METHODS

Design and FEM

Figure 1 shows the design of the electrodes: two small electrodes on the front and back, which are connected to the same signal wire; two bigger measuring electrodes, which are each connected to a single signal wire; one large high voltage electrode. The highest density of the electric field is reached in between the parallel 6 mm gap (see Fig. 1b).

Signal Evaluation

The three raw signals can be used to calculate the xy-coordinates. The transformation (Eq. 1) can be written within a matrix quite similar to the Clarke-transformation [6],

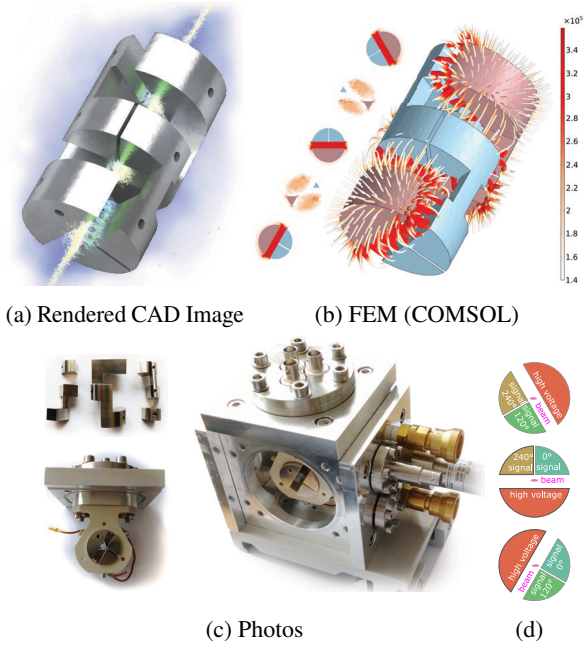

(a) Rendered CAD Image (b) FEM (COMSOL)

(c) Photos (d)

Figure 1: (a) expected location of gas-ions (*light-yellow*), trajectory of free electrones (*lightblue*) (b) electrostatic: measuring electrodes (blue), HV electrode (red), tube-thickness and color: electric field strength [V m^{-1}] (d) signal and HV connections.

which is well-known in electromechanical theory. The values of u, v and w are normalized, taking into account the sum of all intensities. The values c_i are fixed calibration parameters. They can be obtained by linear optimization using measured data.

$$\begin{bmatrix} x \\ y \end{bmatrix} = \begin{bmatrix} c_{x0} & c_{x1} & c_{x2} & c_{x3} \\ c_{y0} & c_{y1} & c_{y2} & c_{y3} \end{bmatrix} \cdot \begin{bmatrix} 1 \\ u \\ v \\ w \end{bmatrix} \tag{1a}$$

$$u = \frac{I_A}{I_A+I_B+I_C} \qquad v = \frac{I_B}{I_A+I_B+I_C} \qquad w = \frac{I_C}{I_A+I_B+I_C} \tag{1b}$$

Signal-Position Calibration

For the calibration several tuples $\langle u_i, v_i, w_i, x_i, y_i, p_i \rangle$ are needed. They have to include the three measure signal values and the corresponding true real x and y positions. Weighting or proportional factors $p_i(x, y)$ assure that some regions will be taken more into account than others. For both algorithms five or more linear independent point assignments are needed. More values will improve the precision of calibration.

Calibration Method I: Simplex-algorithm including weighted residuals To calculate the different coefficients c_*, a Simplex-algorithm was applied. All examples are shown for the y-axis. x-coordinate will be calculated similar to the procedure shown in that chapter. The expression x in

* marcel.goerlitz@desy.de

ISBN: 978-3-95450-229-5 ISSN: 2673-5520 doi:10.18429/JACoW-MEDSI2020-WEPA09

this part corresponds to a vector containing the calibration-coefficients. Calculation can be done by available programs like *Matlab*, where the minimization problem is described as in Eq. (2) [7].

$$\min_x \left(\boldsymbol{f}^T \cdot \boldsymbol{x}\right) \qquad \left\{ \boldsymbol{x} \;\middle|\; \begin{matrix} \boldsymbol{A}_{con} \cdot \boldsymbol{x} & \leq & \boldsymbol{b}_{con} \\ \boldsymbol{A}_{eq} \cdot \boldsymbol{x} & = & \boldsymbol{b}_{eq} \end{matrix} \right\} \tag{2}$$

Note: Column-vectors: bold lowercase letters; matrices: bold capital letters

In order to use the linear optimization the corresponding fixed matrices $\boldsymbol{A}_{con}, \boldsymbol{b}_{con}, \boldsymbol{A}_{eq}$ and $\boldsymbol{b}_{eq}$ have to be expressed in the right way, as it is shown in the following. First of all, new variables will be introduced in Eq. (3).

$$\boldsymbol{T} = \begin{bmatrix} 1 & u_1 & v_1 & w_1 \\ 1 & u_2 & v_2 & w_2 \\ \vdots & \vdots & \vdots & \vdots \\ 1 & u_k & v_k & w_k \end{bmatrix} \boldsymbol{y}_{pos} = \begin{bmatrix} y_{pos\,0} \\ y_{pos\,1} \\ \vdots \\ y_{pos\,k} \end{bmatrix} \boldsymbol{c} = \begin{bmatrix} c_{y0} \\ c_{y1} \\ c_{y2} \\ c_{y3} \end{bmatrix} \boldsymbol{p} = \begin{bmatrix} p_1 \\ p_2 \\ \vdots \\ p_k \end{bmatrix} \tag{3}$$

The vector $\boldsymbol{y}_{pos}$ contains the expected y-Positions. The vector $\boldsymbol{p}$ comprises weight factors for each residuum Δy_i. The calibration coefficients in the vector $\boldsymbol{c}$ are unknown and have to be calculated. The standard problem would be solved like in Eq. (4a). Due to the fact that the right inner part can contain positive as well as negative errors the problem has to be extended by a trick: $\Delta\boldsymbol{y}$ will be replaced by a difference expression, in Eq. (4b), such that errors reached from positive and negative sites are taken into consideration. The constraint in Eq. (4a) implicates that the offset c_0 is taken into account, in a way that the optimum will be found where signal values u, v and w have almost the same value.

$$\begin{aligned} \Delta\boldsymbol{y} &= |\, \boldsymbol{T} \cdot \boldsymbol{c} - \boldsymbol{y} \,| \text{ with } \Delta y > 0 && \text{(4a)} \\ (\Delta\boldsymbol{y}_+ - \Delta\boldsymbol{y}_-) &= \boldsymbol{T} \cdot \boldsymbol{c} - \boldsymbol{y}_{pos} && \text{(4b)} \\ \Leftrightarrow \quad \boldsymbol{y}_{pos} &= \boldsymbol{T}\boldsymbol{c} - \Delta\boldsymbol{y}_+ + \Delta\boldsymbol{y}_- && \text{(4c)} \\ \boldsymbol{b}_{eq} &= \boldsymbol{A}_{eq}\boldsymbol{x} && \text{(4d)} \\ \text{Further constraints } (con): \quad & \Delta\boldsymbol{y}_+,\ \Delta\boldsymbol{y}_- \geq 0 && \text{(4e)} \\ & c_0 = c_1 + c_2 + c_3 && \text{(4f)} \end{aligned}$$

To express Eq. (4c) in the form of Eq. (4d), the vectors and matrices will be described as in Eq. (5). The constraints-Eq. (4f) is expressed in Eq. (5b). The transposed vector of weight factors $\boldsymbol{p}^T$ emphasizes the most significant data point errors. To calculate x the simplex algorithm is used and calculated like it is described in Eq. (2).

$$\boldsymbol{A}_{eq} = \begin{bmatrix} \boldsymbol{T} & -\boldsymbol{I} & \boldsymbol{I} \\ \boldsymbol{C}_{con} & 0 & 0 \end{bmatrix} \quad \boldsymbol{b}_{eq} = \begin{bmatrix} \boldsymbol{y}_{pos} \\ 0 \end{bmatrix} \tag{5a}$$

$$\text{with } \boldsymbol{C}_{con} = \begin{bmatrix} -1 & 1 & 1 & 1 \end{bmatrix} \tag{5b}$$

$$\boldsymbol{A}_{con} = \begin{bmatrix} 0 & 0 & 0 \\ 0 & -\boldsymbol{I} & 0 \\ 0 & 0 & -\boldsymbol{I} \end{bmatrix} \quad \boldsymbol{b}_{con} = \begin{bmatrix} 0 \\ 0 \\ 0 \end{bmatrix} \quad \boldsymbol{x} = \begin{bmatrix} \boldsymbol{c} \\ \Delta\boldsymbol{y}_+ \\ \Delta\boldsymbol{y}_- \end{bmatrix} \tag{5c}$$

$$\boldsymbol{f}^T = \begin{bmatrix} 0 & \boldsymbol{p}^T & \boldsymbol{p}^T & \end{bmatrix} \tag{5d}$$

Calibration Method II: the pseudo-inverse including weighted residuals An alternative solution for the calculation is to use a approximative solution with help of a pseudo-inverse. The Moore-Penrose pseudoinverse notation has to be taken into account to solve a non-quadratic matrix, which will result in a problem like it is described in (6d).

The description of the matrix A and the vector b is as shown in Eq. (6d). The inner matrices $\boldsymbol{T}$, $\boldsymbol{y}_{pos}$ and $\boldsymbol{c}$ are described in Eq. (3). The diagonal matrix $\boldsymbol{D}$ contains the weighting coefficients p_i on the diagonal. The inner product of the hermetic matrix $\boldsymbol{A}^T\boldsymbol{A}$ could be calculated manually by Singular Value Decomposition. Software like Matlab calculate the pseudoinverse directly [8]. After the successful calculation of the pseudo-inverse $\boldsymbol{A}^+$, it just has to be multiplied by $\boldsymbol{b}$ to obtain the vector $\boldsymbol{x}$ [Eq. (6b)], which contains the sought coefficients.

$$\begin{aligned} \boldsymbol{A}\boldsymbol{x} &= \boldsymbol{b} && \text{(6a)} \\ \boldsymbol{x} &\approx \boldsymbol{A}^+ \cdot \boldsymbol{b} && \text{(6b)} \\ \boldsymbol{x} &\approx (\boldsymbol{A}^T\boldsymbol{A})^{-1}\boldsymbol{A}^T \cdot \boldsymbol{b} && \text{(6c)} \end{aligned}$$

$$\boldsymbol{A} = \begin{bmatrix} \boldsymbol{T} & -\boldsymbol{I} \\ 0 & \boldsymbol{D} \end{bmatrix} \quad \boldsymbol{b} = \begin{bmatrix} \boldsymbol{y}_{pos} \\ 0 \end{bmatrix} \quad \boldsymbol{x} = \begin{bmatrix} \boldsymbol{c} \\ \Delta\boldsymbol{y} \end{bmatrix} \tag{6d}$$

RESULTS

First measurements were taken at the DESY-beamline P64 [9] at 20 keV, the chamber was filled with 100 % Nitrogen at atmospheric pressure. Figure 2a shows the measured raw signals, which were obtained by moving the BPM with xz-linear-stage in front of a stable beam. Calibration coefficients were computed by using a mesh of 31x30 different support

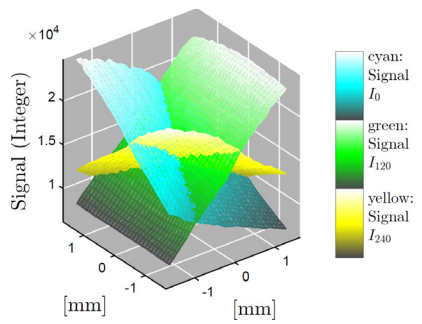

(a) raw signals of the current amplifier:
xy-beam position ↦ electrode raw signals

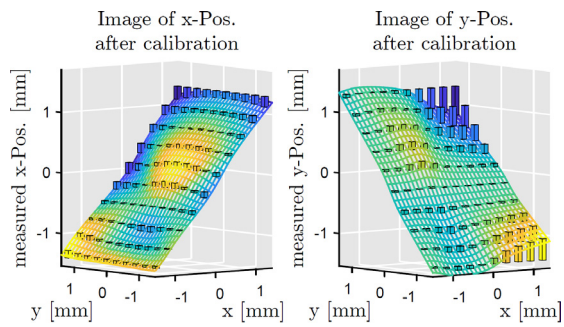

(b) *xy*-beam position ↦ measured (calibrated) value
bar/color: difference to the calibration function

Figure 2: Plots: a N_2-filled chamber was moved along x and y in front of a 0.5x0.5 mm^2 small 20 keV x-ray beam, 31x30 points were taken.

ISBN: 978-3-95450-229-5 ISSN: 2673-5520 doi:10.18429/JACoW-MEDSI2020-WEPA09

Table 1: Calibration Coefficients of Different Beam Sizes - 31x30 datapoints have been used, beamsize was defined by slits alignment. Beamsize before slits was approximately 0.7 mmx1.5 mm

Coefficients	Beamsize [mm] 0.5 x 0.5		0.5 x 1.0		0.5 x 1.5		0.5 x 2.0		1.0 x 2.0		1.0 x 0.5	
	Method I	Method II	Method I	Method II	Method I	Method II	Method I	Method II	Method I	Method II	Method I	Method II
c_{x0}	−0.18	−0.19	−0.16	−0.17	−0.17	−0.18	−0.17	−0.18	−0.25	−0.26	−0.27	−0.27
c_{x1}	−2.73	−2.71	−2.75	−2.74	−2.79	−2.78	−2.79	−2.78	−2.82	−2.81	−2.78	−2.77
c_{x2}	5.07	4.97	5.14	5.06	5.19	5.11	5.22	5.15	5.22	5.16	5.10	5.01
c_{x3}	−2.52	−2.45	−2.55	−2.49	−2.58	−2.52	−2.60	−2.55	−2.65	−2.60	−2.58	−2.51
c_{y0}	−0.17	−0.18	−0.17	−0.18	−0.18	−0.18	−0.15	−0.16	−0.15	−0.15	−0.17	−0.17
c_{y1}	−5.89	−5.96	−5.96	−6.04	−5.99	−6.10	−6.00	−6.14	−6.05	−6.19	−5.92	−6.01
c_{y2}	−0.09	−0.07	−0.11	−0.08	−0.11	−0.07	−0.11	−0.10	−0.11	−0.10	−0.09	−0.07
c_{y3}	5.81	5.85	5.89	5.94	5.92	5.99	5.96	6.08	6.00	6.14	5.84	5.90

points, and a 2d-Gauss weighting. They are shown in Table 1 for different slits openings. One can see that the ratio of coefficients stay almost constant even with different beam sizes. Nevertheless there is a small upscaling, as when the beam-size gets larger. Values show a strictly monotonic behaviour in both directions. For this reason the chamber can be used for position control in further steps.

DISCUSSION

Using one single high voltage electrode and only three signals instead of four might reduce noise failures, particullary because the measured current of an ionization chamber is in the µA to nA-range. Moreover, the design and distribution of electric stray field might be improved by different gap ratios or by redesigning the electrodes gap with an acute instead of a right angle.

Concerning the calibration: The errors between measurement and calibration function are around 0.15 mm in an area 1x1 mm^2 and 0.40 mm in an area of 3x3 mm^2. Improvements can be reached by a higher-order polynomial regression. In addition, there exist other methods, like least-square-optimization or gradient-based optimization. However, the shown methods do not require start parameters and is well suited for small problems. On the contrary data points have to be injective [10] and the problem has to be linear.

CONCLUSION

A new concept of a beam position monitor using three signals to determine a 2d-position has been presented. After the calibration, position data shows a linear behaviour. The basic idea opens possibilities for new types of beam position monitors. The chamber can find application at beamlines, where BPM diffraction peaks have to be avoided or absorption behaviour need to be changed easily.

The calibration was validated by the comparison of two different methods, which lead to similar results. These methods have been explained in detail to give a comprehensive overview. They can be applied to other unknown linear systems as well, like mechanical multi-sensor-positioning systems, mixed signal measurements etc.

ACKNOWLEDGEMENTS

Special acknowledge goes to the DESY-workshop, the CNC preparation group and to the P64 staff: Akhil Tayal, Vadim Murzin, Maria Naumova, Aleksandr Kalinko.

REFERENCES

[1] E. Griesmayer, P. Kavrigin, Ch. Weiss, and C. Bloomer, "The Use of Single-crystal CVD Diamond as a Position Sensitive X-ray Detector", in *Proc. 5th Int. Beam Instrum. Conf. (IBIC'16)*, Barcelona, Spain, Sep. 2016, pp. 71–74. doi:10.18429/JACoW-IBIC2016-MOPG14

[2] M. Marinelli, E. Milani, *et al.*, " X-ray beam monitor made by thin-film CVD single-crystaldiamondr", *J. Synchrotron Rad.*, vol. 19, pp. 1015–1020, Nov. 2012. doi:10.1107/S0909049512038186

[3] A.N. Fisenkoa, A.V. Kosova, *et al.*, "Coordinate-sensitive ionization chamber with highspatial resolution", *Nucl. Instrum. Methods A*, vol. 543, no. 1, pp. 361–364, May 2005. doi:10.1016/j.nima.2005.01.256

[4] K. Sato,"A position-sensitive ionization chamber for XAFS studies at synchrotron sources", *J. Synchr. Radiat.*, vol. 8, pp. 378-80, 2001. doi:10.1107/s0909049500015855

[5] K. Sato, H. Toyowaka *et al.*, "The Behavior of Ionization Chambers under the Irradiation of High Flux X-Ray Beam", SPring-8, Hyogo, Japan, 1998.

[6] Edith Clarke, *Circuit Analysis of AC Power Systems. Vol. I.* New York, NY, USA: J. Wiley & sons, 1943.

[7] https://www.mathworks.com/help/optim/ug/linear-programming-algorithms.html

[8] https://de.mathworks.com/help/matlab/ref/pinv.html

[9] W.A. Caliebe, V. Murzin, A. Kalinko, and M. Görlitz, "High-flux XAFS-beamline P64 at PETRA III", *AIP Conference Proceedings*, vol. 2054, p. 060031, 2019. doi:10.1063/1.5084662

[10] https://mathworld.wolfram.com/Injection.html